Optimal incident energy of heavy ion fusion

Reddi Rani L. [1], N. Sowmya [2,*], H. C. Manjunatha, [3,†] K. N. Sridhar [3,4] and M. M. Armstrong Arasu[1]

[1]*Department of Physics, St. Joseph's College (Autonomous), Affiliated to Bharathidasan University, Tiruchirappalli, 620002 TN, India*
[2]*Department of Physics, Government First Grade College, Chikkaballapur-562101, Karnataka, India*
[3]*Department of Physics, Government First Grade College, Devanahalli-562110, Karnataka, India*
[4]*Department of Physics, Government First Grade College, Malur-563160, Karnataka, India*

We systematically explored all conceivable combinations of projectiles and targets through experimental studies, focusing on the synthesis of lanthanides to superheavy nuclei within the atomic number range of $58 \leqslant Z \leqslant 117$. Utilizing the dinuclear system model, we evaluated evaporation residue cross sections for each fusion reaction, identified optimal energies associated with larger evaporation residue cross sections. Our study delved into the influence of entrance channel parameters such as mass asymmetry, charge asymmetry, charge product, Coulomb interaction parameter, mean fissility, and fusion barrier height on these optimal energies. Notably, a systematic variation in optimal energies was observed for the Coulomb interaction parameter. Additionally, the deformation parameter exhibited an influence on optimal energies, and pronounced discrepancies were noted in specific fusion reactions such as ^{40}Ar(^{181}Ta, $4n$) ^{217}Pa, and for the reactions such as ^{16}O(^{134}Ba, $4n$) ^{146}Gd, ^{4}He(^{166}Er, $3n$) ^{167}Yb, and ^{48}Ca(^{249}Bk, $4n$) ^{293}Ts, when compared to other fusion reactions explored. The empirical formula presented successfully replicates experimental optimal energies for the atomic number range $58 \leqslant Z \leqslant 117$. Its straightforward application involves inputting the atomic and mass numbers of the projectile and target nuclei, along with deformation parameters, underscoring its simplicity and effectiveness in predicting optimal energies in diverse fusion reactions. This simplicity underscores the predictive power of the proposed formula, offering a valuable tool for understanding and predicting optimal energies in a wide range of fusion reactions involving lanthanides and superheavy nuclei.

I. INTRODUCTION

Superheavy elements are extremely heavy chemical elements with atomic numbers greater than 103. These elements are characterized by their very unstable nuclei due to the large number of protons and neutrons they contain. Superheavy elements are typically produced in nuclear reactions [1–3] and have very short half-lives [1,4,5], often on the order of milliseconds or even microseconds. These elements are typically created by bombarding heavy target nuclei with accelerated beams of lighter nuclei in particle accelerators [6–8]. The resulting collisions can lead to the formation of new, heavier elements. The superheavy elements are identified by their decay products [9,10].

Further, the role of optimal energies in the synthesis of superheavy elements is crucial to the success of creating these extremely heavy and unstable elements in the laboratory [11–14]. Choosing optimal energies to synthesize superheavy elements is a critical aspect of experimental nuclear physics. It involves precise control of the energy of colliding nuclei to overcome the Coulomb barrier and maximize the probability of successful fusion reactions,

ultimately leading to the creation and identification of these short-lived, heavy elements. A compromise between higher incident energy and lower compound nucleus excitation reveals an optimum condition, yielding enhanced residue cross sections in specific channels under certain cooling and fissioning conditions [15]. Superheavy element 117 synthesis is analyzed [16], with ^{48}Ca + ^{249}Bk identified as an optimal combination. The ^{48}Ca(^{250}Bk, $4n$) ^{294}Ts reaction is hindered experimentally. Evaporation residue cross sections depend exponentially on fission and neutron emission saddle point mass difference, emphasizing isotopic composition importance. Entrance channel effects favor ^{48}Ca + ^{245}Bk over ^{50}Ti + ^{243}Am and ^{55}Mn + ^{238}U. Further, Li *et al.*, [17] proposed dynamic theory for superheavy element, treating fusion and fission consistently through a time-dependent diffusion equation in collective coordinate space.

Synthesizing eighth-period elements faces challenges due to quasifission. Experimental analysis indicates that deformation parameters play a major role, surpassing entrance channel criteria. Five rules, including optimal beam energy selection, are proposed as guidelines for superheavy element synthesis [11]. Wada *et al.* [18] proposed a diffusion model for superheavy element synthesis, employing a one-dimensional Smoluchowski equation with a liquid drop model potential, incorporating temperature-dependent shell correction energy. Competition between fission and neutron evaporation,

influenced by temperature, yields an optimum evaporation residue cross section. The isotope dependence is notable, favoring neutron-rich compounds with small neutron separation energy. Heavy ion fusion reactions are critical for synthesizing superheavy elements. The proper selection of entrance channels and optimal beam energies is crucial [13] and the study reveals improper beam energy choices contributed to low production cross sections, hindering measurement success. A dynamical model based on the dinuclear system concept [19] is proposed to describe superheavy nuclei formation in complete fusion reactions, incorporating relative motion and nucleon transfer. Systematic investigations of cold fusion reactions provide insight into isotopic trends, proposing optimal combinations and excitation energies for synthesizing superheavy elements $Z = 110, 112, 114, 116, 118$, and 120.

A comprehensive investigation focused on identifying projectile-target combinations and predicting optimal energies that yield larger production cross sections. The studies employed detailed analysis to determine the most suitable conditions for achieving enhanced outcomes in terms of cross-sectional production in the superheavy region [20–23]. In-depth investigations into optimal energies for heavy and superheavy elements inspired the formulation of a semiempirical formula. Integrating experimental data and an advanced statistical model, our proposed formula aims to provide a comprehensive and accurate framework for predicting outcomes in heavy and superheavy element synthesis.

II. THEORETICAL FRAMEWORK

The evaporation residue cross sections in the atomic number region $58 \leqslant Z \leqslant 117$ were evaluated using the dinuclear system model. The evaporation residue cross sections were evaluated as follows:

$$\sigma_{ER}^{\mathrm{DNS},xn} = \sum_{\ell=0}^{\infty} (2\ell + 1)\sigma_{\mathrm{fus}}^{\mathrm{DNS}}(E_{\mathrm{c.m.}})P_{sur}^{xn}(E^*, l). \quad (1)$$

The symbol $\sigma_{\mathrm{fus}}^{\mathrm{DNS}}$ denotes the partial fusion cross section, signifying the probability of nuclei transitioning beyond the Coulomb barrier to form a dinuclear system (DNS). This occurs as the kinetic energy $E_{\mathrm{c.m.}}$ and angular momentum ℓ of relative motion convert into the excitation energy and angular momentum of the DNS. $\sigma_{\mathrm{fus}}^{\mathrm{DNS}}$ is given by

$$\sigma_{\mathrm{fus}}^{\mathrm{DNS}}(E^*, l) = \sigma_{cap}(E_{\mathrm{c.m.}})P_{CN}^{\mathrm{DNS}}(E^*, l). \quad (2)$$

The compound nucleus formation probability $P_{CN}^{\mathrm{DNS}}(E^*, l)$ is expressed as

$$P_{CN}^{\mathrm{DNS}} = \frac{\rho(E_{\mathrm{DNS}}^* - B_{\mathrm{fus}}^*)}{\rho(E_{\mathrm{DNS}}^* - B_{\mathrm{fus}}^*) + \rho(E_{\mathrm{DNS}}^* - B_{qf})}. \quad (3)$$

Here, ρ is the level density and it is a function of B_{qf}, B_{fus}^*, and E_{DNS}^*, where B_{qf} is the barrier of the nucleus-nucleus interaction potential, which must overcome if the dinuclear system decays into two fragments. B_{fus}^* is the intrinsic fusion barrier which is determined by the difference between the maximum of a driving potential and its value at the point corresponding to the initial charge asymmetry of the considered fusion reaction. Further, E_{DNS}^* is the excitation energy of the dinuclear system given by the difference between beam

energy and a minimum of nucleus-nucleus potential ($E_{\mathrm{DNS}}^* = E_{\mathrm{c.m.}} - V_m$) [24]. Here, V_m is the minimum of the nucleus-nucleus potential. The term B_{qf}, B_{fus}^*, and E_{DNS}^* is evaluated using nucleus-nucleus potential energy [25] which is defined as follows:

$$V(R, Z_1, Z_2, \beta_{2i}, l) = V_c(R, Z_1, Z_2, \beta_{2i})$$
$$+ V_N(R, Z_1, Z_2, \beta_{2i}) + V_{\mathrm{rot}}(l, \beta_{2i}), \quad (4)$$

where V_C, V_N, and V_{rot} are the Coulomb, nuclear, and rotational potentials, respectively. The Coulomb potential is given by

$$V_C(R, Z_1, Z_2, \beta_{2i}) = \frac{Z_1 Z_2}{R}e^2 + \frac{Z_1 Z_2}{R^3}e^2$$
$$\times \left[\left(\frac{9}{20\pi}\right)^{1/2} \sum_{i=1}^{2} R_i^2 \beta_{2i} P_2(\cos\alpha_i) \right.$$
$$\left. + \frac{3}{7\pi} \sum_{i=1}^{2} R_i^2 [\beta_{2i} P_2(\cos\alpha_i)]^2 \right]. \quad (5)$$

Z_1 and Z_2 are the charges of the nuclei forming the DNS. P_2 is the Legendre polynomial of the nuclei forming the DNS. The nuclear potential is defined as

$$V_N(R, Z_1, Z_2, \beta_{2i}) = V_o \left\{ \exp\left[\frac{-2(R - R_{12})\alpha}{R_{12}}\right] \right.$$
$$\left. - 2\exp\left[\frac{-(R - R_{12})\alpha}{R_{12}}\right] \right\}. \quad (6)$$

Here, V_o is the strength of the potential, α is the mass asymmetry, and the quantity R_{12} is determined by

$$R_{12} = D_1 + D_2 + 0.1\,\mathrm{fm}, \quad (7)$$

where

$$D_i(i = 1, 2) = R_i \left[1 + \left(\frac{5}{4\pi}\right)^{1/2} \beta_{2i} - \frac{1}{4\pi}\beta_{2i}^2 \right]. \quad (8)$$

The quantity α used in Eq. (6) is given by

$$\alpha = (11.47 - 17.32a_1a_2 + 2.07\overline{R}_0) \left[1 + 0.25 \sum_{i=1}^{2} \beta_{2i} \right]. \quad (9)$$

The quantity $\overline{R}_0$ is defined as follows:

$$\overline{R}_0 = \frac{R_1 R_2}{R_1 + R_2}. \quad (10)$$

The rotational potential of the DNS is defined as

$$V_{\mathrm{rot}}(R, l, \beta_{2i}) = \frac{\hbar^2 \ell(\ell + 1)}{2\Im_{\mathrm{DNS}}(R, A, \beta_{2i})}, \quad (11)$$

where ℓ is the angular momentum and $\Im_{\mathrm{DNS}}$ is the moment of inertia of the DNS. The driving potential is written as

$$U(Z, A, R) = V(R, Z_1, Z_2, \beta_{2i}, l) - Q \quad (12)$$

and the mass excess energy Q is as

$$Q = B_1(Z_1) + B_2(Z_2) - B_{CN}(Z_{CN}). \quad (13)$$
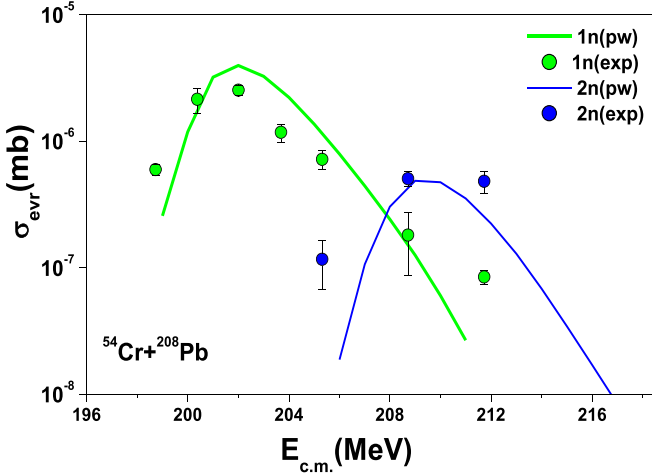
FIG. 1. A plot of evaporation residue cross sections of $^{54}Cr + ^{208}Pb$ for $1n$ and $2n$ channel as a function of center of mass energy. A hollow sphere with green and blue fill corresponds to the experimental values. A continuous line specifies the values obtained using the present work.

The binding energies, denoted as $B_1(Z_1)$, $B_2(Z_2)$, and $B_{CN}(Z_{CN})$, represent the ground state binding energies of fragments in the DNS, as well as that of the compound nucleus. These values are sourced from [26].

III. RESULTS AND DISCUSSIONS

We initially investigated all projectile-target combinations available through experiments, forming lanthanides to super-heavy nuclei within the atomic number range $58 \leqslant Z \leqslant 117$. Further, using the DNS model, we evaluated evaporation residue cross sections of all experimentally available fusion reactions as explained in theory section.

In the investigation of fusion reactions, optimal energies are critical for achieving larger evaporation residue cross sections. For the $^{54}Cr + ^{208}Pb$ fusion reaction, the evaporation residue cross section was studied. Experimental results, depicted in Fig. 1, revealed a maximum cross section of 2.52 nb at 202.01 MeV, compared to the theoretical value of 3.73 nb at the same energy. Additionally, the $2n$ channel exhibited a noteworthy cross section of 0.504 nb at 208.72 MeV with
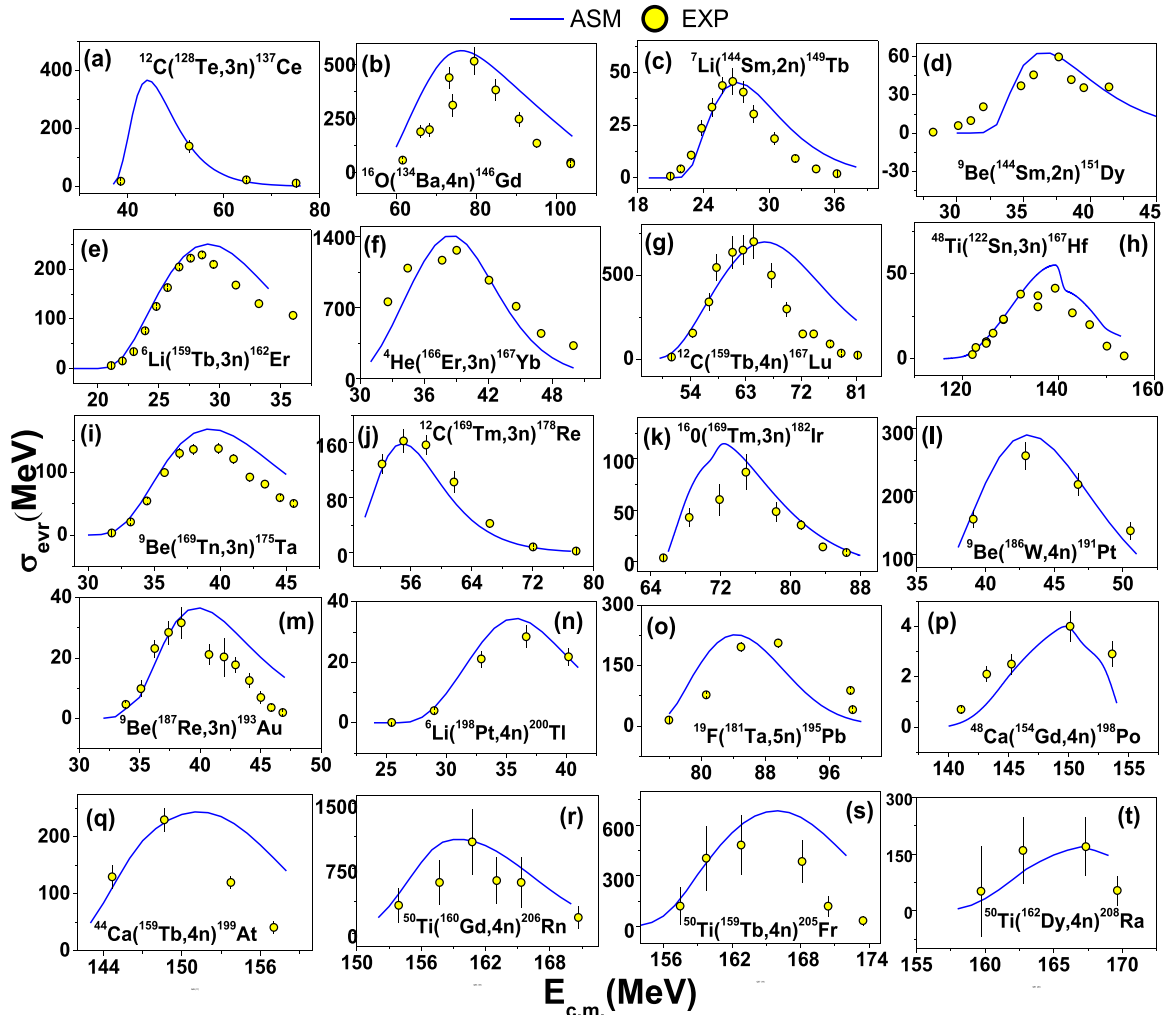

FIG. 2. A plot of evaporation residue cross-sections of fusion reactions leading to form (a) ^{140}Ce to (s) ^{209}Fr for a particular channel for which a larger cross section is observed. Other details are similar to Fig. 1.
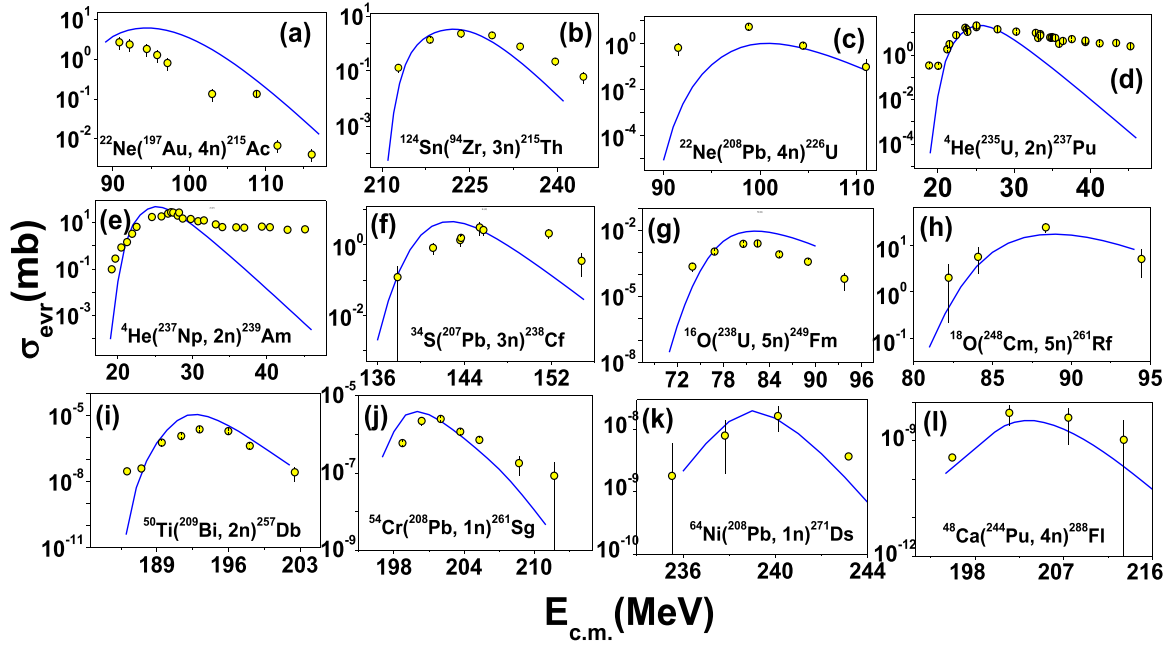
FIG. 3. A plot of evaporation residue cross-sections of fusion reactions leading to form (a) ^{219}Ac to (s) ^{292}Fl for a particular channel for which a larger cross section is observed. Other details are similar to Fig. 1.

a corresponding theoretical value of 0.46 nb. Remarkably, both experimental and theoretical assessments consistently identified 202.01 MeV as the optimal energy, yielding larger cross sections. Accordingly, this energy corresponding to a larger cross section is considered as optimal energy. Hence, the optimal energy refers to the point where the highest observed evaporation residue cross-sections occur. It signifies the energy level at which the fusion reaction is most efficient in producing evaporation residues, providing insights into the optimal conditions for synthesizing heavy nuclei in nuclear experiments.

By employing this approach, we determined the optimal energies for all fusion reactions documented in the literature, encompassing the formation of isotopes from ^{140}Ce to ^{209}Fr (Fig. 2) and ^{219}Ac to ^{292}Fl (Fig. 3). In majority of cases, we noticed larger cross sections both experimentally and theoretically. However, a discrepancy of about 10 MeV is observed in the case of predicted optimal energy using the present model. Which also results in an order of magnitude of evaporation residue cross sections. In all these investigated fusion reactions, we noticed optimal energy at which a larger evaporation residue cross section is observed experimentally. Further, to construct an empirical formula, we investigated entrance channel parameters. The effect of entrance channel parameters on fusion reactions is a critical aspect as it determines the primary influence among entrance channel parameters on optimal energies, highlighting the key factors governing the success of fusion reactions.

Entrance channel parameters such as mass symmetry $(\eta_A = |\frac{A_1 - A_2}{A_1 + A_2}|)$, charge asymmetry $(\alpha_Z = |\frac{Z_1 - Z_2}{Z_1 + Z_2}|)$, charge product $(Z_1 Z_2)$, Coulomb interaction parameter $(Z_{\text{Coul}} = \frac{Z_1 Z_2}{A_1^{1/3} + A_2^{1/3}})$, mean fissility $(\chi_m = 0.25\chi_{CN} + 0.75\chi_{\text{eff}})$,

where $\chi_{CN} = \frac{Z^2/A}{\chi} = \frac{Z^2/A}{50.883[1-1.7826(\frac{A-2Z}{A})^2]}$ and $\chi_{\text{eff}} = \frac{\frac{4Z_1 Z_2}{(A_1^{1/3} + A_2^{1/3}) \times (A_1 A_2)^{1/3}}}{50.883[1-1.7826(\frac{A-2Z}{A})^2]}$, and fusion barrier height (V_B) have been investigated. Figures 4(a)–4(f) shows a plot of optimal energy as a function of different entrance channel parameters. When compared to mass and charge asymmetry, optimal energy shows systematic variation for charge product, Coulomb interaction parameters, χ_m, and fusion barrier height. In order to assess this systematic variation, a linear equation was fitted, aiming for a maximum coefficient of determination ($R^2 \approx 1$), as discussed in [27]. Notably, while the coefficient of determination is maximized for various entrance channel parameters such as $Z_1 Z_2$, Z_{Coul}, χ_m, and V_B, the analysis reveals that Z_{Coul} exhibits the highest coefficient of determination, reaching $R^2 = 0.993$. Hence, a fitted equation for optimal energy as a function of Z_{Coul} is as follows:

$$E_{\text{opt}}(\text{MeV}) = 6.2555 - 0.9998 \times Z_{\text{Coul}}. \qquad (14)$$

Here, $Z_{\text{Coul}} = \frac{Z_1 Z_2}{A_1^{1/3} + A_2^{1/3}}$.

Influence of deformation parameter on optimal energy

Further, we investigated the influence of the deformation parameter on optimal energy. To verify the influence of the deformation parameter on optimal energy, we tried many functions such as $Z_{\text{Coul}} + (\exp\beta_{2P} + \exp\beta_{2T})$, $Z_{\text{Coul}}(\exp\beta_{2P} + \exp\beta_{2T} + \exp\beta_{2C})$, $Z_{\text{Coul}}\exp(\beta_{2P} + \beta_{2T})$, $Z_{\text{Coul}} + (\exp\beta_{2P} + \beta_{2T})$, $Z_{\text{Coul}}(\exp\beta_{2P} + \exp\beta_{2T})$, $Z_{\text{Coul}}\exp(\beta_{2P} + \beta_{2T} + \beta_{2C})$, and $Z_{\text{Coul}} + \ln(\beta_{2P} + \beta_{2T}) + \exp(A_1 + A_2)$ and so on. Among all the investigated functions,
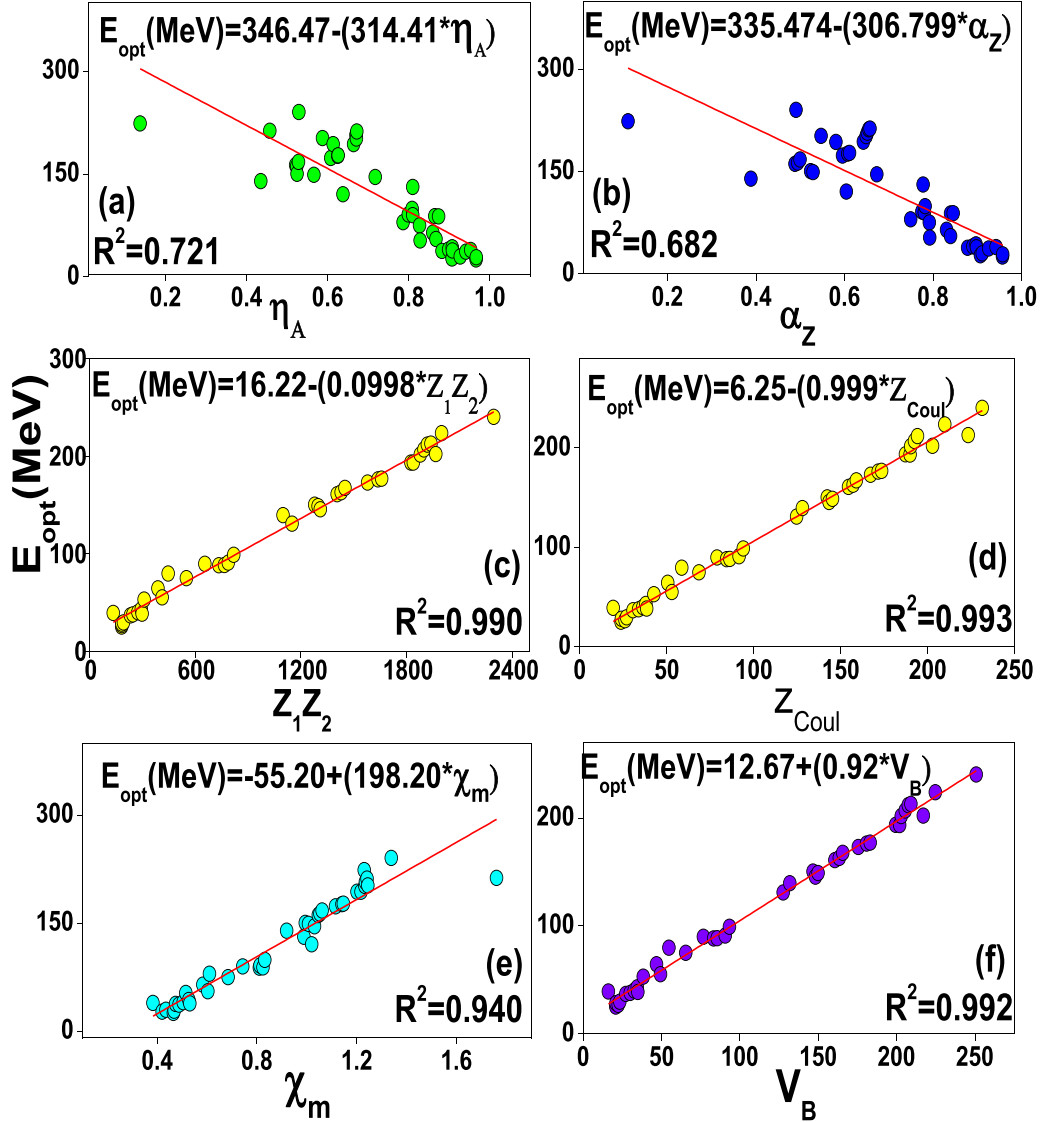
FIG. 4. A plot of optimal energies of fusion reactions leading to form ^{141}Ce to ^{292}Fl as a function of (a) mass asymmetry, (b) charge asymmetry, (c) charge product, (d) Coulomb interaction parameter, (e) mean fissility, and (f) fusion barrier height.

the function $Z_{\text{Coul}} + (\exp \beta_{2P} + \exp \beta_{2T})$ shows a systematic variation and coefficient of determination is increased from 0.993 to 0.996 (see Fig. 5). The best fitted equation for optimal energy is as follows:

$$E_{\text{opt}} = 0.79 + 1.025 \times [Z_{\text{Coul}} + (\exp \beta_{2P} + \exp \beta_{2T})]. \quad (15)$$

Here, β_{2P} and β_{2T} are quadrupole deformation parameters of projectile and target nuclei. Hence, variations in the deformation parameter were found to significantly impact the optimal energy levels, providing insights into the relationship between structural deformations and the energy requirements for achieving optimal outcomes. Further, we tabulated experimental optimal energy and optimal energy obtained using Eqs. (14) and (15) in Table I. From this table it is inferred that the optimal energy obtained using Eqs. (15) and (14)

are in good agreement with experimental values. However, a deviation of about 10 MeV is observed in case of fusion reactions such as ^{16}O(^{134}Ba, $4n$) ^{146}Gd, ^{4}He(^{166}Er, $3n$) ^{167}Yb, ^{40}Ar(^{181}Ta, $4n$) ^{217}Pa, and ^{48}Ca(^{249}Bk, $4n$) ^{293}Ts which is also in concurrence with the earlier studies [12].

Further, we investigated the $E_{\text{opt}}^{\text{exp}} - E_{\text{opt}}$ for assessing the accuracy and consistency of the proposed empirical formula for optimal energy. Hence, $E_{\text{opt}}^{\text{exp}} - E_{\text{opt}}$ plotted as a function of Z_{Coul} and it is shown in Fig. 6. The difference in the predicted and experimental optimal energy lies between ± 10 MeV for the majority of cases. However, the difference in the energy is found to be larger by about 30 MeV for the fusion reaction of ^{40}Ar $+ \ ^{181}$Ta, and for the reactions such as ^{16}O $+ \ ^{134}$Ba, ^{4}He $+ \ ^{166}$Er, and ^{48}Ca $+ \ ^{249}$Bk the predicted energy varies between 13 to 20 MeV.
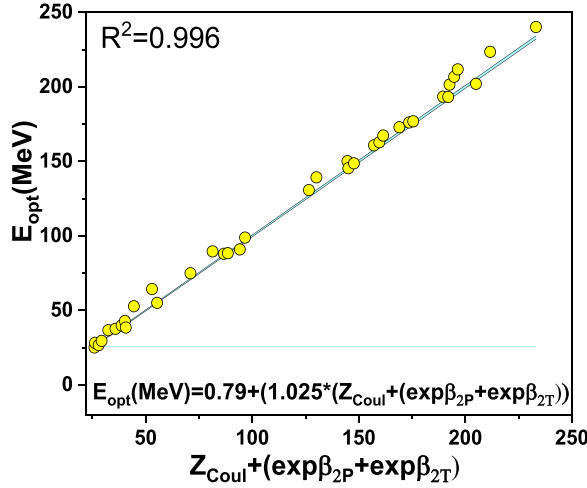
FIG. 5. A plot of optimal energy as a function of $Z_{Coul} + (\exp \beta_{2P} + \exp \beta_{2T})$.

IV. SUMMARY

We investigated all possible projectile-target combinations available through experiments forming lanthanides to superheavy nuclei in the atomic number range $58 \leqslant Z \leqslant 117$. The evaporation residue cross sections have been evaluated using the dinuclear system model. For each fusion reaction, optimal energy is identified corresponding to larger evaporation residue cross sections. Further, the effect of entrance channel parameters such as mass asymmetry, charge asymmetry, charge product, Coulomb interaction parameter, mean fissility, and fusion barrier height has been studied on optimal energies. Optimal energies show systematic variation for the Coulomb interaction parameter. Further, we noticed an influence of the deformation parameter on optimal energies. The larger deviation of about 13 to 30 MeV were observed for ^{40}Ar(^{181}Ta, $4n$)^{221}Pa, and for the reactions such as ^{16}O(^{134}Ba, $4n$)^{150}Gd, ^{4}He(^{166}Er, $3n$)^{170}Yb, and ^{48}Ca(^{249}Bk, $4n$) when compared to other fusion reactions in-
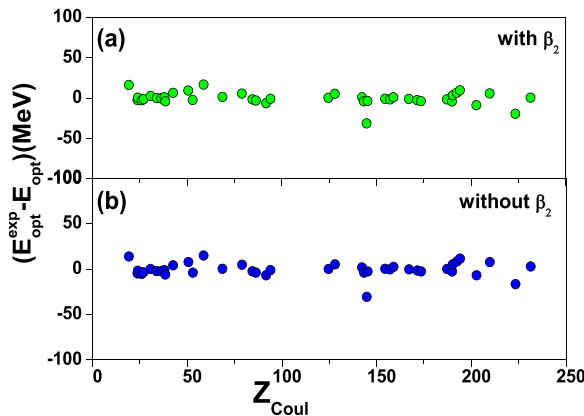

FIG. 6. A plot of the difference in experimental optimal energy and optimal energy predicted from present work as a function of Z_{Coul} using (a) with deformations and (b) without deformations of projectile and target nuclei.

TABLE I. A tabulation of fusion reactions, fusion barrier height, optimal energies obtained using experimental result, with deformations [Eq. (15)] and without deformations [Eq. (14)].

	V_B	E_{opt}(MeV)		
Compound nucleus	MeV	exp	Eq. (15)	Eq. (14)
^{12}C(^{128}Te, $3n$) ^{137}Ce [28]	38.4	52.8	46.4	48.8
^{16}O(^{134}Ba, $4n$) ^{146}Gd [29]	54.8	79.5	63.0	64.9
^{7}Li(^{144}Sm, $2n$) ^{149}Tb [30]	22.4	26.7	29.5	32.3
^{9}Be(^{144}Sm, $2n$) ^{151}Dy [31]	30.0	37.6	38	40.1
^{6}Li(^{159}Tb, $3n$) ^{162}Er [32]	23.4	29.5	31	33.2
^{4}He(^{166}Er, $3n$) ^{167}Yb [33]	16.2	39.0	23.0	25.5
^{12}C(^{159}Tb, $4n$) ^{167}Lu [34]	46.8	64.3	55.1	56.9
^{48}Ti(^{122}Sn, $3n$) ^{167}Hf [35]	132.0	139.3	134.2	134.2
^{9}Be(^{169}Tm, $3n$) ^{175}Ta [36]	32.6	39.9	40.5	42.5
^{12}C(^{169}Tm, $3n$) ^{178}Re [28]	49.3	55.1	57.6	59.2
^{16}O(^{169}Tm, $3n$) ^{182}Ir [28]	65.6	74.9	73.6	74.83
^{9}Be(^{186}W, $4n$) ^{191}Pt [37]	34.5	42.9	42.1	44.3
^{9}Be(^{187}Re, $3n$) ^{193}Au [36]	35.0	38.4	42.5	44.7
^{6}Li(^{198}Pt, $4n$) ^{200}Tl [38]	27.2	36.7	34.1	36.9
^{19}F(^{181}Ta, $5n$) ^{195}Pb [39]	76.8	89.6	84.3	85.2
^{48}Ca(^{154}Gd, $4n$) ^{198}Po [40]	146.8	150.1	149.1	148.5
^{44}Ca(^{159}Tb, $4n$) ^{199}At [41]	150.0	148.7	152.2	151.5
^{50}Ti(^{160}Gd, $4n$) ^{206}Rn [42]	160.7	160.8	161.8	161
^{50}Ti(^{159}Tb, $4n$) ^{205}Fr [42]	163.6	162.8	164.4	163.3
^{50}Ti(^{162}Dy, $4n$) ^{208}Ra [42]	165.7	167.3	166.3	165.2
^{22}Ne(^{197}Au, $4n$) ^{215}Ac [43]	90.8	90.8	97.3	97.9
^{124}Sn(^{94}Zr, $3n$) ^{215}Th [44]	224.8	223.5	217.7	216.0
^{40}Ar(^{181}Ta, $4n$) ^{217}Pa [45]	149.7	120.3	151.6	151.0
^{22}Ne(^{208}Pb, $4n$) ^{226}U [43]	93.4	98.8	99.9	100.2
^{4}He(^{235}U, $2n$) ^{237}Pu [45]	20.8	25.1	27.4	30.0
^{4}He(^{237}Np, $2n$) ^{239}Am [46]	21.0	28.2	27.7	30.2
^{34}S(^{207}Pb, $3n$) ^{238}Cf [47]	148.2	145.4	149.5	149.5
^{48}Ca(^{197}Au, $2n$) ^{243}Es [48]	175.7	172.9	174.1	173.4
^{16}O(^{238}U, $2n$) ^{252}Fm [49]	83.3	88.0	89.7	90.7
^{48}Ca(^{208}Pb, $2n$) ^{254}No [47]	181.0	176.07	178.7	177.8
^{48}Ca(^{209}Bi, $2n$)^{255}Lr [48]	183.2	176.8	180.7	179.7
^{18}O(^{248}Cm, $5n$)^{261}Rf [50]	85.6	88.4	91.6	92.5
^{50}Ti(^{209}Bi, $5n$)^{254}Db [51]	202.0	193.2	198	196.1
^{54}Cr(^{208}Pb, $1n$)^{261}Sg [52]	217.1	202.0	210.9	209.0
^{26}Mg(^{248}Cm, $1n$)^{273}Hs [53]	127.8	130.7	130.6	130.8
^{64}Ni(^{208}Pb, $1n$)^{271}Ds [54]	251.0	240.1	239.7	237.6
^{48}Ca(^{238}U, $3n$)^{283}Cn [55]	199.4	193.8	195.0	193.4
^{48}Ca(^{244}Pu, $3n$)^{289}Fl [55]	203.1	201.5	198.2	196.4
^{48}Ca(^{243}Am, $3n$)^{288}Mc [55]	205.6	206.8	200.4	198.6
^{48}Ca(^{245}Cm, $3n$)^{290}Lv [55]	207.6	211.7	202.2	200.3
^{48}Ca(^{249}Bk, $4n$)^{293}Ts [55]	209.2	212.7	232.1	229.5

vestigated. Hence, the proposed empirical formula reproduces experimental optimal energies in the atomic number range $58 \leqslant Z \leqslant 117$ with the simple input of an atomic and mass number of a projectile and target nuclei in addition to defor-

mation parameters. This simplicity underscores the predictive power of the proposed formula, offering a valuable tool for understanding and predicting optimal energies in a wide range of fusion reactions involving lanthanides and superheavy nuclei.

[1] Y. Oganessian, Synthesis and decay properties of superheavy elements, Pure Appl. Chem. **78**, 889 (2006).

[2] Y. T. Oganessian, A. V. Yeremin, A. G. Popeko, S. L. Bogomolov, G. V. Buklanov, M. L. Chelnokov, V. I. Chepigin, B. N. Gikal, V. A. Gorshkov, G. G. Gulbekian *et al.*, Synthesis of nuclei of the superheavy element 114 in reactions induced by ^{48}Ca, Nature (London) **400**, 242 (1999).

[3] S. Hofmann, Synthesis and properties of superheavy elements, Radiochimica Acta **84**, 121 (1999).

[4] P. Roy Chowdhury, C. Samanta, and D. N. Basu, α decay half-lives of new superheavy elements, Phys. Rev. C **73**, 044911 (2006).

[5] S. Hofmann, Properties and Syntheses of Superheavy Elements, in *The Chemistry of Superheavy Elements* (Springer, Berlin, 2003), pp. 1–29.

[6] Y. T. Oganessian and V. K. Utyonkov, Superheavy nuclei from ^{48}Ca-induced reactions, Nucl. Phys. A **944**, 62 (2015).

[7] Z.-Q. Feng, G.-M. Jin, J.-Q. Li, and W. Scheid, Production of heavy and superheavy nuclei in massive fusion reactions, Nucl. Phys. A **816**, 33 (2009).

[8] Y. T. Oganessian, Synthesis and decay properties of heaviest nuclei with ^{48}Ca-induced reactions, Nucl. Phys. A **787**, 343 (2007).

[9] K. Moody *et al.* (Dubna-Livermore Collaboration), Superheavy element isotopes, decay properties, Nucl. Phys. A **734**, 188 (2004).

[10] P. Armbruster, On the production of superheavy elements, Annu. Rev. Nucl. Part. Sci. **50**, 411 (2000).

[11] H. C. Manjunatha, Y. S. Vidya, P. S. Damodara Gupta, N. Manjunatha, N. Sowmya, L. Seenappa, and T. Nandi, Rules of thumb for synthesizing superheavy elements, J. Phys. G: Nucl. Part. Phy. **49**, 125101 (2022).

[12] L. Zhu, Law of optimal incident energy for synthesizing superheavy elements in hot fusion reactions, Phys. Rev. Res. **5**, L022030 (2023).

[13] H. C. Manjunatha, N. Sowmya, P. S. Damodara Gupta, L. Seenappa, and T. Nandi, Role of optimal beam energies in the heavy ion fusion reaction, Eur. Phys. J. Plus **137**, 693 (2022).

[14] L. Zhu, W.-J. Xie, and F.-S. Zhang, Production cross sections of superheavy elements z = 119 and 120 in hot fusion reactions, Phys. Rev. C **89**, 024615 (2014).

[15] Y. Aritomo, T. Wada, M. Ohta, and Y. Abe, Fluctuation-dissipation model for synthesis of superheavy elements, Phys. Rev. C **59**, 796 (1999).

[16] Z. H. Liu and J.-D. Bao, Optimal reaction for synthesis of superheavy element 117, Phys. Rev. C **80**, 034601 (2009).

[17] F. Li, L. Zhu, Z.-H. Wu, X.-B. Yu, J. Su, and C.-C. Guo, Predictions for the synthesis of superheavy elements z=119 and 120, Phys. Rev. C **98**, 014618 (2018).

[18] T. Wada, Y. Aritomo, T. Tokuda, M. Ohta, and Y. Abe, Dynamics of the superheavy element synthesis with a diffusion model, Nucl. Phys. A **616**, 446 (1997).

[19] Z.-Q. Feng, G.-M. Jin, J.-Q. Li, and W. Scheid, Formation of superheavy nuclei in cold fusion reactions, Phys. Rev. C **76**, 044606 (2007).

[20] H. C. Manjunatha, K. N. Sridhar, and N. Sowmya, Investigations of the synthesis of the superheavy element z=122, Phys. Rev. C **98**, 024308 (2018).

[21] H. C. Manjunatha, N. Sowmya, N. Manjunatha, P. S. Damodara Gupta, L. Seenappa, K. N. Sridhar, T. Ganesh, and T. Nandi, Entrance channel dependent hot fusion reactions for superheavy element synthesis, Phys. Rev. C **102**, 064605 (2020).

[22] N. Sowmya, H. C. S. Manjunatha, P. S. S. D. Gupta, L. Seenappa, N. Manjunatha, and T. Ganesh, Optimizing ^{45}Sc induced fusion reactions to synthesis superheavy elements, J. Phys. Soc. Jpn. **92**, 074201 (2023).

[23] H. C. Manjunatha, P. S. Damodara Gupta, N. Sowmya, and K. N. Sridhar, Investigations on ^{48}Ca and ^{58}Fe-induced heavy ion fusion reactions, Int. J. Mod. Phys. E **31**, 2250015 (2022).

[24] G. Giardina, S. Hofmann, A. I. Muminov, and A. K. Nasirov, Effect of the entrance channel on the synthesis of superheavy elements, Euro. Phys. J. A **8**, 205 (2000).

[25] S. Soheyli and M. Varasteh Khanlari, Theoretical study of effects of the entrance channel on the relative yield of complete fusion and quasifission in heavy-ion collisions within a dinuclear system approach, Phys. Rev. C **94**, 034615 (2016).

[26] G. Audi, A. H. Wapstra, and C. Thibault, The AME2003 atomic mass evaluation: (II). Tables, graphs and references, Nucl. Phys. A **729**, 337 (2003).

[27] H. C. Manjunatha, P. S. Damodara Gupta, N. Sowmya, N. Manjunatha, K. N. Sridhar, L. Seenappa, and T. Nandi, Survival probability of compound nuclei in heavy-ion fusion reaction, J. Phys. G: Nucl. Part. Phys. **50**, 035101 (2023).

[28] M. K. Sharma, P. P. Singh, D. P Singh, A. Yadav, V. R. Sharma, I. Bala, R. Kumar, B. P. Singh, R. Prasad *et al.*, Systematic study of pre-equilibrium emission at low energies in ^{12}C-and ^{16}O-induced reactions, Phys. Rev. C **91**, 014603 (2015).

[29] S. Della Negra, H. Gauvin, H. Jungclas, Y. Le Beyec, and M. Lefort, Comparison between experimental decay of the compound nuclei ^{150}Gd and evaporation calculations, Z. Phys. A **282**, 75 (1977).

[30] P. K. Rath, S. Santra, N. L. Singh, B. K. Nayak, K. Mahata, R. Palit, K. Ramachandran, S. K. Pandit, A. Parihari, A. Pal *et al.*, Complete fusion in ^{7}Li + ^{144,152}Sm reactions, Phys. Rev. C **88**, 044617 (2013).

[31] P. R. S. Gomes, I. Padron, E. Crema, O. A. Capurro, J. O. Fernández Niello, A. Arazi, G. V. Martí, J. Lubian, M. Trotta, A. J. Pacheco *et al.*, Comprehensive study of reaction mechanisms for the ^{9}Be + ^{144}Sm system at near-and sub-barrier energies, Phys. Rev. C **73**, 064606 (2006).

[32] P. R. S. Gomes, I. Padron, E. Crema, O. A. Capurro, J. O. FernandezNiello, A. Arazi, G. V. Marti, J. Lubian, M. Trotta, A. J. Pacheco, J. E. Testoni, M. D. Rodriguez, M. E. Ortega, L. C. Chamon, R. M. Anjos, R. Veiga, M. Dasgupta, D. J. Hinde, and K. Hagino, Phys. Rev. C **83**, 064606 (2011).

[33] S. Gil, R. Vandenbosch, A. Charlop, A. Garca, D. D. Leach, S. J. Luke, and S. Kailas, Spin distribution of the compound nucleus formed by ^{16}O + ^{154}Sm, Phys. Rev. C **43**, 701 (1991).

[34] A. Yadav, V. R. Sharma, P. P. Singh, D. P. Singh, M. K. Sharma, Unnati Gupta, R. Kumar, B. P. Singh, R. Prasad, and R. K.

Bhowmik, Large influence of incomplete fusion in ^{13}C + ^{159}Tb at $E_{lab} \sim$ 4–7 MeV/nucleon, Phys. Rev. C **85**, 034614 (2012).

[35] S. Gil, F. Hasenbalg, J. E. Testoni, D. Abriola, M. C. Berisso, M. di Tada, A. Etchegoyen, J. O. Fernández Niello, A. J. Pacheco, A. Charlop, A. A. Sonzogni, and R. Vandenbosch, Fusion cross sections in systems leading to ^{170}Hf at near-barrier energies, Phys. Rev. C **51**, 1336 (1995).

[36] Y. D. Fang, P. R. S. Gomes, J. Lubian, M. L. Liu, X. H. Zhou, D. R. Mendes Junior, N. T. Zhang, Y. H. Zhang, G. S. Li, J. G. Wang, S. Guo, Y. H. Qiang, B. S. Gao, Y. Zheng, X. G. Lei, and Z. G. Wang, Complete and incomplete fusion of ^{9}Be + ^{169}Tm, ^{187}Re at near-barrier energies, Phys. Rev. C **91**, 014608 (2015).

[37] Y. D. Fang, P. R. S. Gomes, J. Lubian, X. H. Zhou, Y. H. Zhang, J. L. Han, M. L. Liu, Y. Zheng, S. Guo, J. G. Wang, Y. H. Qiang, Z. G. Wang, X. G. Wu, C. Y. He, Y. Zheng, C. B. Li, S. P. Hu, and S. H. Yao, Fusion and one-neutron stripping reactions in the ^{9}Be + ^{186}W system above the Coulomb barrier, Phys. Rev. C **87**, 024604 (2013).

[38] Y. E. Penionzhkevich, S. M. Lukyanov, R. A. Astabatyan, N. A. Demekhina, M. P. Ivanov, R. Kalpakchieva, A. A. Kulko, E. R. Markaryan, V. A. Maslov, Y. A. Muzychka *et al.*, Complete and incomplete fusion of ^{6}Li ions with Bi and Pt, J. Phys. G: Nucl. Part. Phys. **36**, 025104 (2009).

[39] D. J. Hinde, J. R. Leigh, J. O. Newton, W. Galster, and S. Sie, Fission and evaporation competition in ^{200}Pb, Nucl. Phys. A **385**, 109 (1982).

[40] D. A. Mayorov, T. A. Werke, M. C. Alfonso, M. E. Bennett, and C. M. Folden III, Production cross sections of elements near the n = 126 shell in ^{48}Ca-induced reactions with ^{154}Gd, ^{159}Tb, ^{162}Dy, and ^{165}Ho targets, Phys. Rev. C **90**, 024602 (2014).

[41] T. A. Werke, D. A. Mayorov, M. C. Alfonso, E. E. Tereshatov, and C. M. Folden III, Hot fusion-evaporation cross sections of ^{44}Ca-induced reactions with lanthanide targets, Phys. Rev. C **92**, 054617 (2015).

[42] D. A. Mayorov, T. A. Werke, M. C. Alfonso, E. E. Tereshatov, M. E. Bennett, M. M. Frey, and C. M. Folden III, Evaporation residue excitation function measurements in ^{50}Ti- and ^{54}Cr-induced reactions with lanthanide targets, Phys. Rev. C **92**, 054601 (2015).

[43] A. N. Andreev, D. D. Bogdanov, A. V. Eremin, A. P. Kabachenko, O. A. Orlova, G. M. Ter-Akop'yan, and V. I. Chepigin, Measurement of cross sections for reactions with evaporation of light particles in the complete fusion channel in bombardment of Au and Pb by Ne ions, Sov. J. Nucl. Phys. **50**, 1989 (1989).

[44] K. H. Schmidt, P. Armbruster, F. P. Hessberger, G. Münzenberg, W. Reisdorf, C. C. Sahm, D. Vermeulen, H. G. Clerc, J. Keller, and H. Schulte, The barrier for compound-nucleus formation in the nearly symmetric systems ^{86}Kr + ^{123}Sb ^{209}Fr and ^{124}Sn + ^{94}Zr ^{218}Th, Z. Phys. A **301**, 21 (1981).

[45] D. Vermeulen, H. G. Clerc, C. C. Sahm, K. H. Schmidt, J. G. Keller, G. Münzenberg, and W Reisdorf, Cross sections for evaporation residue production near the n = 126 shell closure, Z. Phys. A **318**, 157 (1984).

[46] A. Fleury, F. H. Ruddy, M. N. Namboodiri, and John M Alexander, Excitation functions for spallation products and fission isomers in ^{237}Np (^{4}He, xn) $^{241-x}$Am reactions, Phys. Rev. C **7**, 1231 (1973).

[47] Y. T. Oganessian, V. K. Utyonkov, Y. V. Lobanov, F. S. Abdullin, A. N. Polyakov, I. V. Shirokovsky, Y. S. Tsyganov, A. N. Mezentsev, S. Iliev, V. G. Subbotin, A. M. Sukhov, K. Subotic, O. V. Ivanov, A. N. Voinov, V. I. Zagrebaev, K. J. Moody, J. F. Wild, N. J. Stoyer, M. A. Stoyer, and R. W. Lougheed, Measurements of cross sections for the fusion-evaporation reactions ^{204,206,207,208}Pb + ^{48}Ca and ^{207}Pb^{34}S: Decay properties of the even-even nuclides ^{238}Cf and ^{250}No, Phys. Rev. C **64**, 054606 (2001).

[48] H. W. Gäggeler, D. T. Jost, A. Türler, P. Armbruster, W. Brüchle, H. Folger, F. P. Heßberger, S. Hofmann, G. Münzenberg, V. Ninov *et al.*, Cold fusion reactions with ^{48}Ca, Nucl. Phys. A **502**, 561 (1989).

[49] K. Nishio, H. Ikezoe, Y. Nagame, M. Asai, K. Tsukada, S. Mitsuoka, K. Tsuruta, K. Satou, C. J. Lin, and T. Ohsawa, Evidence of complete fusion in the sub-barrier ^{16}O + ^{238}U reaction, Phys. Rev. Lett. **93**, 162701 (2004).

[50] M. Murakami, S. Goto, H. Murayama, T. Kojima, H. Kudo, D. Kaji, K. Morimoto, H. Haba, Y. Kudou, T. Sumita *et al.*, Excitation functions for production of Rf isotopes in the ^{248}Cm + ^{18}O reaction, Phys. Rev. C **88**, 024618 (2013).

[51] S. Hofmann, F. P. Heßberger, D. Ackermann, G. Münzenberg, S. Antalic, P. Cagarda, B. Kindler, J. Kojouharova, M. Leino, B. Lommel *et al.*, New results on elements 111 and 112, Eur. Phys. J. A: Hadrons Nucl. **14**, 147 (2002).

[52] M. G. Itkis, S. Beghini, A. A. Bogachev, L. Corradi, O. Dorvaux, A. Gadea, G. Giardina, F. Hanappe, I. M. Itkis, M. Jandel *et al.*, Shell effects in fission and quasi-fission of heavy and superheavy nuclei, Nucl. Phys. A **734**, 136 (2004).

[53] J. Dvorak, W. Bruchle, M. Chelnokov, C. E. Dullmann, Z. Dvorakova, K. Eberhardt, R. Eichler, E. Jager, R. Krucken, A. Kuznetsov, Y. Nagame, F. Nebel, K. Nishio, R. Perego, Z. Qin, M. Schadel, B. Schausten, E. Schimpf, R. Schuber, A. Semchenkov, P. Thorle, A. Turler, M. Wegrzecki, B. Wierczinski, A. Yakushev, and A. Yeremin, Observation of the 3n evaporation channel in the complete hot-fusion reaction ^{26}Mg + ^{248}Cm leading to the new superheavy nuclide ^{271}Hs, Phys. Rev. Lett. **100**, 132503 (2008).

[54] K. Morita, K. K. Morimoto, D. Kaji, S. Goto, H. Haba, E. Ideguchi, R. Kanungo, K. Katori, H. Koura, H. Kudo *et al.*, Status of heavy element research using Garis at RIKEN, Nucl. Phys. A **734**, 101 (2004).

[55] Y. T. Oganessian and V. K. Utyonkov, Super-heavy element research, Rep. Prog. Phys. **78**, 036301 (2015).